Two-photon production WW pair at the LHC.

A. Manko, R. Shulyakovsky

Institute of Physics, National Academy of Sciences of Belarus
68 Nezavisimosti av., Minsk, 220072, Belarus,
Institute of Apply Physics, National Academy of Sciences of Belarus
16 Academicheskay st., Minsk, 220072, Belarus

Minsk 2023

Major task

Our major task is to calculate total and differential cross sections for process $pp \to p + W^- W^+ + p$ at LHC, where W boson decays in leptonic and hadron channels for the leading order and the next-to-leading order. These processes can be used to search the effects of “new physics”. The parton's process of process $pp \to p + W^- W^+ + p$ is the process $\gamma\gamma \to W^- W^+$. The monte carlo generator TwoPhotonGen is used to calculate the total and differential cross sections for process $\gamma\gamma \to W^- W^+$.r FastJet is used to calculate jets from the W boson hadronic channel decay. Pythia is used to calculate channels of decay of W boson. LoopTools is used to calculate one-loop integrals.

Feynman diagrams and the amplitude of the process $\gamma\gamma \to W^- W^+$

The following diagram of the processes: $pp \to pW^- W^+ p$ is shown in elastic case: where $P1$ and $P2$ – 4–momentum of initial hadrons, $P1'$ and $P2'$ – 4–momentum of final hadrons of W bosons, $k1$ and $k2$ – 4–momentum of W^- and W^+ corresponding.

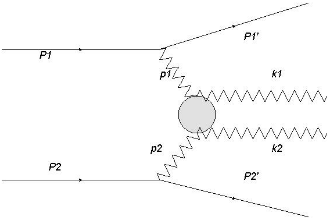

Figure 1: The diagram of the two–photon production the WW pair at LHC

Leading Order

The following diagram of the subprocesses is shown in the leading order:

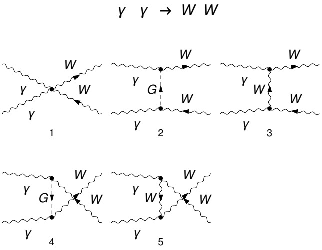

Figure 2: The diagrams of the subprocess in the leading order

Feynman diagrams and the amplitude of the process $\gamma\gamma \to W^- W^+$

Next–Leading Order

There ate 144 self-energies diagrams. The one of these diagrams is shown at this figure.

$$\gamma \quad \gamma \quad \rightarrow \quad W \quad W$$

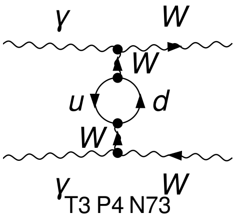

Figure 3: The self–energy diagrams of the subprocess in the next–leading order

Next–Leading Order

There ate 137 boxes diagrams. The one of these diagrams is shown at this figure.

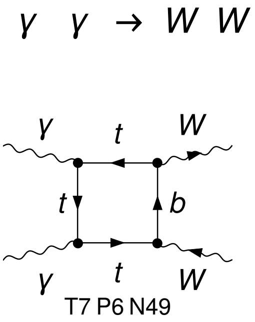

Figure 4: The boxes diagram of the subprocess in the next–to–leading order

Next–Leading Order

There ate 402 boxes diagrams. The one of these diagrams is shown at this figure.

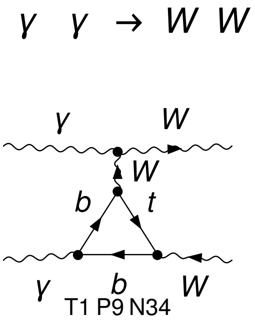

Figure 5: The vertex diagram of the subprocess in the next–to–leading order

Feynman diagrams and the amplitude of the process $\gamma\gamma \to \gamma W^- W^+$

Next–Leading Order

There are 30 hard bremsstrahlung diagrams in the leading order. The hard bremsstrahlung diagram of the subprocesses is shown in the figure.

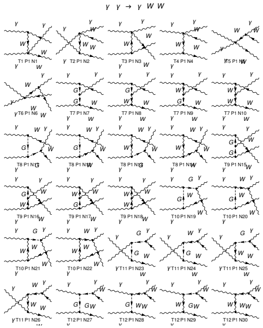

Figure 6: The hards diagrams of the subprocess in the leading order

The approximation of Weizsacker-Williams(parametrization Budnev and Ginsburg[V.M. Budnev et al., Phys.Rep. 15C (1975) 181]) is used to obtain of total and differential cross sections for the two–photon production lepton pairs. The distribution of photon for protons is given:

$$f_p(x) = \frac{\alpha}{\pi x}\left(1 - \frac{1}{x}\right)\left(\varphi\left(\frac{q^2_{max}}{q^2_0}\right) - \varphi\left(\frac{q^2_{min}}{q^2_0}\right)\right), \quad (1)$$

where function φ is

$$\varphi(\xi) = (1+ay)\left(\sum_{k=1}^{3}\frac{1}{k(1+\xi)^k} - \ln(1+\xi^{-1})\right) - \frac{(1-b)y}{4\xi(1+\xi)^3} + c$$
$$\left(1+\frac{y}{4}\right)\left(\ln\left[\frac{1+\xi-b}{1+\xi}\right] + \sum_{k=1}^{3}\frac{b^k}{k(1+\xi)^k}\right), \quad (2)$$

where: $a = 7.16$, $b = -3.96$, $c = 0.028$, $q^2_0 = 0.71\,GeV^2$, $q^2_{max} = 2$, $q^2_{min} = \frac{m_p^2 x^2}{1-x}$, $y = \frac{x^2}{(1-x)}$.

Parametrization

We used Mandelstam variables for a description of the square modulus of the matrix elements of the investigated process, total and differential cross sections. The amplitudes and diagrams of the matrix element were obtained in the program Mathematica using the package FeynArts 3.9. The square module matrix element was obtained in the program Mathematica using the package FormCalc 9.10.

Regularization and renormalization for process $\gamma\gamma \to W^- W^+$

The dimensional regularization developed by 't Hooft[G. 't Hooft, 1971, Nucl. Phys. B33, 173] and Veltman[G. 't Hooft, M Velman 1972, Nucl. Phys. B44, 189] and the scheme of renormalization developed by A. Denner[A. Denner, Fortsch. Phys. 1993 41, №4 307] were used to calculate the UV- and IR-finite amplitudes. The packages LoopTools was used to calculate numerical loops integrals.

Cuts for the process $\gamma\gamma \to W^- W^+$

The cuts for ATLAS shown at table 1 were used to calculate total and differential cross section.

Cut	Value
m_{ll}	$>=$ 20 GeV
p_{T_l}	$>=$ 12 GeV
p_{T_j}	$>=$ 12 GeV
$\lvert\eta_l\rvert$	$<$ 2.4
$\lvert\eta_j\rvert$	$<$ 2.4
ΔR_{ll}	$>$ 0.4
ΔR_{jj}	$>$ 0.4
Forward detector: $\lvert\eta_p\rvert$	$4.3 < \lvert\eta_p\rvert < 4.9$

Table 1: The cuts for ATLAS

LHC: total cross section: $pp \to p + W^- W^+ + p \to p + e^- \bar{\nu}_e e^+ \nu_e + p$

The total cross section in the elastic case for hadrons colliders is given:

$$\sigma(s) = \int dx_1 \int dx_2 f_p(x_1) f_{p)}(x_2) \hat{\sigma}(x_1 x_2 s). \qquad (3)$$

There are results of total cross section of the process $pp \to p + W^- W^+ + p \to p + e^- \bar{\nu}_e e^+ \nu_e + p$ for the leading and the next–to–leading order at LHC at the elastic case at the table 2.

Collider	LO σ pb	NLO σ pb
LHC $\sqrt{s} = 7$ TeV	$3.816 \cdot 10^{-4}$	$3.159 \cdot 10^{-4}$
LHC $\sqrt{s} = 8$ TeV	$4.516 \cdot 10^{-4}$	$3.719 \cdot 10^{-4}$
LHC $\sqrt{s} = 13$ TeV	$6.523 \cdot 10^{-4}$	$6.338 \cdot 10^{-4}$
LHC $\sqrt{s} = 14$ TeV	$7.719 \cdot 10^{-4}$	$6.785 \cdot 10^{-4}$

Table 2: Total Cross sections

LHC: total cross section: $pp \to p + W^- W^+ + p \to p + \mu^- \bar{\nu}_\mu \mu^+ \nu_\mu + p$

There are results of total cross section of the process $pp \to p + W^- W^+ + p \to p + \mu^- \bar{\nu}_\mu \mu^+ \nu_\mu + p$ for the leading and the next–to–leading order at LHC at the elastic case at the table 3.

Collider	LO σ pb	NLO σ pb
LHC $\sqrt{s} = 7$ TeV	$3.816 \cdot 10^{-4}$	$3.158 \cdot 10^{-4}$
LHC $\sqrt{s} = 8$ TeV	$4.516 \cdot 10^{-4}$	$3.719 \cdot 10^{-4}$
LHC $\sqrt{s} = 13$ TeV	$6.523 \cdot 10^{-4}$	$6.338 \cdot 10^{-4}$
LHC $\sqrt{s} = 14$ TeV	$7.719 \cdot 10^{-4}$	$6.785 \cdot 10^{-4}$

Table 3: Total Cross sections

LHC: total cross section: $pp \to p + W^- W^+ + p \to p + e^- \bar{\nu}_e \mu^+ \nu_\mu + p$

There are results of total cross section of the process $pp \to p + W^- W^+ + p \to p + e^- \bar{\nu}_e \mu^+ \nu_\mu + p$ for the leading and the next–to–leading order at LHC at the elastic case at the table 4.

Collider	LO σ pb	NLO σ pb
LHC $\sqrt{s} = 7$ TeV	$3.816 \cdot 10^{-4}$	$3.158 \cdot 10^{-4}$
LHC $\sqrt{s} = 8$ TeV	$4.516 \cdot 10^{-4}$	$3.719 \cdot 10^{-4}$
LHC $\sqrt{s} = 13$ TeV	$6.523 \cdot 10^{-4}$	$6.338 \cdot 10^{-4}$
LHC $\sqrt{s} = 14$ TeV	$7.719 \cdot 10^{-4}$	$6.785 \cdot 10^{-4}$

Table 4: Total Cross sections

LHC: total cross section: $pp \to p + W^- W^+ + p \to p + \mu^- \bar{\nu}_\mu e^+ \nu_e + p$

There are results of total cross section of the process $pp \to p + W^- W^+ + p \to p + \mu^- \bar{\nu}_\mu e^+ \nu_e + p$ for the leading and the next–to–leading order at LHC at the elastic case at the table 5.

Collider	LO σ pb	NLO σ pb
LHC $\sqrt{s} = 7$ TeV	$3.816 \cdot 10^{-4}$	$3.158 \cdot 10^{-4}$
LHC $\sqrt{s} = 8$ TeV	$4.516 \cdot 10^{-4}$	$3.719 \cdot 10^{-4}$
LHC $\sqrt{s} = 13$ TeV	$6.523 \cdot 10^{-4}$	$6.338 \cdot 10^{-4}$
LHC $\sqrt{s} = 14$ TeV	$7.719 \cdot 10^{-4}$	$6.785 \cdot 10^{-4}$

Table 5: Total Cross sections

LHC: total cross section: $pp \to p + W^- W^+ + p \to p + j4 + p$

There are results of total cross section of the process $pp \to p + W^- W^+ + p \to p + j4 + p$ for the leading and the next–to–leading order at LHC at the elastic case at the table 6.

Collider	LO σ pb	NLO σ pb
LHC $\sqrt{s} = 7$ TeV	$4.646 \cdot 10^{-2}$	$4.610 \cdot 10^{-2}$
LHC $\sqrt{s} = 8$ TeV	$6.559 \cdot 10^{-2}$	$6.227 \cdot 10^{-2}$
LHC $\sqrt{s} = 13$ TeV	$2.258 \cdot 10^{-1}$	$2.246 \cdot 10^{-1}$
LHC $\sqrt{s} = 14$ TeV	$2.728 \cdot 10^{-1}$	$2.646 \cdot 10^{-1}$

Table 6: Total Cross sections

The differential cross section as a function of the invariant mass of the $W^- W^+$ for the process $pp \to p + W^- W^+ + p \to p + e^- \bar{\nu}_e e^+ \nu_e + p$ (left) and the process $pp \to p + W^- W^+ + p \to p + e^- \bar{\nu}_e \mu^+ \nu_\mu + p$ (right) are shown at figs 9. The blue line is the leading order and the red line is the next-to-leading order.

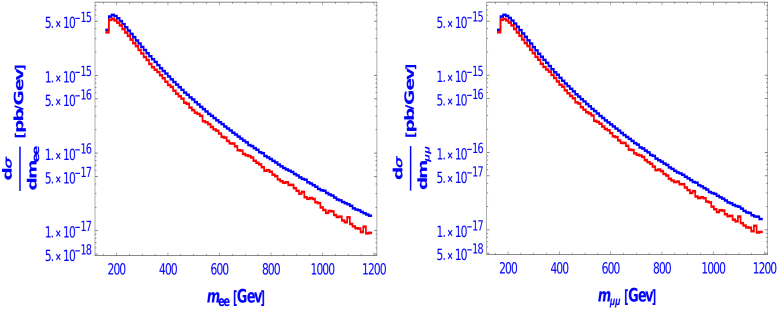

Figure 7: Differential cross section of production in dependence of the invariant mass for elastic case for $\sqrt{s} = 7.0$ TeV.

The differential cross section as a function of the invariant mass of the $W^- W^+$ for the process $pp \to p + W^- W^+ + p \to p + \mu^- \bar{\nu}_\mu e^+ \nu_e + p$ (left) and the process $pp \to p + W^- W^+ + p \to p + \mu^- \bar{\nu}_\mu \mu^+ \nu_\mu + p$ (right) are shown at figs 9. The blue line is the leading order and the red line is the next-to-leading order.

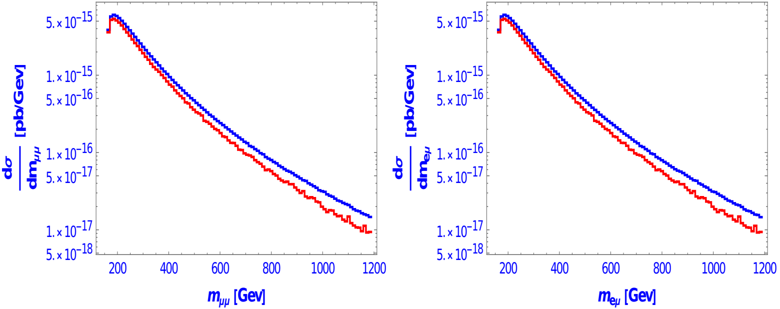

Figure 8: Differential cross section of production in dependence of the invariant mass for elastic case for $\sqrt{s} = 7.0$ TeV.

The differential cross section as a function of the pseudorapdity of electron for the process $pp \to p + W^- W^+ + p \to p + e^- \bar{\nu}_e e^+ \nu_e + p$ (left) and the process $pp \to p + W^- W^+ + p \to p + e^- \bar{\nu}_e \mu^+ \nu_\mu + p$ (right) are shown at figs 9. The blue line is the leading order and the red line is the next-to-leading order.

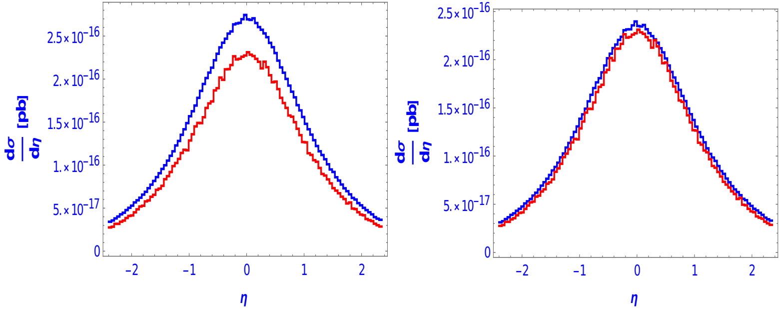

Figure 9: Differential cross section of e^+e^- production in dependence of the pseudorapdity of electron (left) and muon (right) for elastic case for $\sqrt{s} = 7.0$ TeV.

Conclusion

We obtained total and differential cross section in the leading order and the next-to-leaidng order for the process of two–photon production W bosons pair at LHC and decay W boson in leptonic and hadron channels by using the cuts for the final hadrons(leptons). We showed what the process of two–photon creation W bosons pair at LHC can be used to calibrate Luminosity of these colliders and to search ”new physics” at these colliders. Total and differential cross sections for two-photon production of W bosons pairs were studied for elastic case at LHC.

Thank you for your attention!